Gene-expression profiling of different arms of lymphatic vasculature identifies candidates for manipulation of cell traffic

Imtiaz Iftakhar-E-Khuda[a], Ruth Fair-Mäkelä[a], Anu Kukkonen-Macchi[a], Kati Elima[a,b], Marika Karikoski[a], Pia Rantakari[a], Masayuki Miyasaka[a,c], Marko Salmi[a,d], and Sirpa Jalkanen[a,d,1]

[a]MediCity Research Laboratory, University of Turku, 20520 Turku, Finland; [b]Department of Medical Biochemistry and Genetics, University of Turku, 20520 Turku, Finland; [c]World Premier International Immunology Frontier Research Center, Osaka University, 565-0871 Osaka, Japan; and [d]Department of Medical Microbiology and Immunology, University of Turku, 20520 Turku, Finland

Afferent lymphatic vessels bring antigens and diverse populations of leukocytes to draining lymph nodes, whereas efferent lymphatics allow only lymphocytes and antigens to leave the nodes. Despite the fundamental importance of afferent vs. efferent lymphatics in immune response and cancer spread, the molecular characteristics of these different arms of the lymphatic vasculature are largely unknown. The objective of this work was to explore molecular differences behind the distinct functions of afferent and efferent lymphatic vessels, and find possible molecules mediating lymphocyte traffic. We used laser-capture microdissection and cell sorting to isolate lymphatic endothelial cells (LECs) from the subcapsular sinus (SS, afferent) and lymphatic sinus (LS, efferent) for transcriptional analyses. The results reveal marked differences between afferent and efferent LECs and identify molecules on lymphatic vessels. Further characterizations of Siglec-1 (CD169) and macrophage scavenger receptor 1 (MSR1/CD204), show that they are discriminatively expressed on lymphatic endothelium of the SS but not on lymphatic vasculature of the LS. In contrast, endomucin (EMCN) is present on the LS endothelium and not on lymphatic endothelium of the SS. Moreover, both murine and human MSR1 on lymphatic endothelium of the SS bind lymphocytes and in in vivo studies MSR1 regulates entrance of lymphocytes from the SS to the lymph node parenchyma. In conclusion, this paper reports surprisingly distinct molecular profiles for afferent and efferent lymphatics and a function for MSR1. These results may open avenues to explore some of the now-identified molecules as targets to manipulate the function of lymphatic vessels.

lymphatics | cell traffic | lymphocytes | endothelium

L ymphatic vessels have unique functions different from those of blood vessels. These unique characteristics also reflect the preferential expression of certain molecules on lymphatic endothelium versus blood vessel endothelium. Molecules and mechanisms controlling angiogenesis and lymphangiogenesis are extensively studied (1). In contrast, the molecular mechanisms involved in cell entrance via the afferent lymphatics to and their exit from a lymph node (LN) via efferent lymphatics are less well known. Molecules such as lymphatic vessel endothelial hyaluronan receptor-1 (Lyve-1), podoplanin, vascular endothelial growth factor receptor-3 (VEGFR-3), and prospero homeobox 1 (PROX1), which discriminate lymphatic from blood vessel endothelium are expressed at roughly comparable levels both on afferent and efferent lymphatics in human (2). Moreover, molecules known to participate in physiological cell trafficking such as sphingosine-1-phosphate receptor, macrophage mannose receptor, and Clever-1/Stabilin-1 act both on the afferent and efferent arms of the lymphatic vasculature (3–6). Functionally afferent and efferent lymphatics have a fundamental difference: most leukocytes can enter the LN via the afferent lymphatics, but only lymphocytes can exit the nodes via the efferent lymphatics under steady-state conditions. Access to the efferent lymphatics is a major control point both in leukocyte trafficking and tumor spread. This control point decides what type of

immune response is created elsewhere in the body and it also determines what types of cancer cells can leave the draining LN. Even though this phenomenon is well recognized, the molecular mechanisms behind it are completely unknown. Therefore, we used a genome-wide microarray approach followed by expression analyses at the protein level to identify molecules preferentially expressed either on afferent [subcapsular sinus (SS)] or efferent [lymphatic sinus (LS), i.e., cortical and subcortical sinuses] murine lymphatics, and tested these differences in mouse and man. Siglec-1 (CD169) and macrophage scavenger receptor 1 (MSR1/CD204) were found to be present on lymphatic endothelium of the SS, whereas endomucin (EMCN) was found on lymphatic vasculature of the LS. In functional tests, we discovered MSR1-mediated binding between lymphatic MSR1 and lymphocytes and a role for MSR1 in controlling lymphocyte entrance from the SS into the LN parenchyma.

Results

Microarray Analyses Reveal Differentially Expressed Genes Between the Afferent and Efferent Arms of the Lymphatic Vasculature. Two methods, laser capture microdissection (LCM) and cell sorting with flow cytometry, were used to isolate lymphatic endothelial cells (LECs) from the afferent and efferent arms of lymph node lymphatics. For laser microdissection the cells were collected from the SS endothelium and LS endothelium. The harsh procedure (*Methods*) limits the possibilities of using the majority of the antibodies

Significance

This paper elucidates one of the enigmas in immunology: What determines the discriminative traffic via afferent and efferent lymphatics? We report so far unrecognized and vastly distinct molecular profiles of lymphatic endothelial cells (LECs) in the afferent and efferent arms of the lymphatic system in the lymph nodes. Moreover, the work takes three of the hit molecules to more detailed analyses regarding their expression and function, and presents a previously unknown function in regulation of the lymphocyte traffic for macrophage scavenger receptor on LECs of the subcapsular sinus. Importantly, the findings of this work may potentially be exploitable in drug design when searching for new targets to manipulate immune response or cancer spread.

IMMUNOLOGY AND INFLAMMATION

commonly used to identify lymphatics and macrophages. The preliminary testing showed that using CD31 as an endothelial marker and F4/80 as a macrophage marker to discriminate macrophages from lymphatic endothelium is compatible with the applicability of the antibodies for the required conditions (Fig. 1A). Anti-CD31 was used to detect all LECs and F4/80 to detect particularly those macrophages that line the endothelial layer (www.macrophages.com/subcapsular-sinus-lymph-node) in the SS. For cell sorting with flow cytometry the target populations were detected as a lineage$^-$/podoplanin$^+$ population set to comprise 1% of the total digested LN cells based on the previous literature (7). CD73 that is expressed on the SS endothelium but not on the LS endothelium (8) was then used as a marker to sort 12% of the brightest CD73$^+$ (SS endothelial cells) and the dimmest 12% (CD73$^-$ LS endothelial cells) of the cells as shown in Fig. S1.

To compare the LECs at the two arms of the lymphatic vasculature in peripheral lymph nodes in more detail, we performed microarray analyses of the isolated cell populations and studied the differences in transcriptomics between the two groups of cells. The data show that the gene expression signatures of LECs differing in location were clearly distinct (Fig. 1 B and C). The expression of 399 genes, including many long noncoding RNAs (lncRNA), was up-regulated in LS endothelial cells by at least eightfold, whereas 286 genes showed more than eightfold reduction in expression (Figs. S2 and S3 and Table S1). When the differentially expressed genes were further subjected to unbiased annotation enrichment analyses

and functional grouping analyses, several enriched annotations in many categories related to cellular processes and metabolic functions were detected, especially in the down-regulated group of genes. In addition, several categories pointing to stress- and immune responses were enriched (Table S2).

MSR1 and Siglec-1 Are Preferentially Expressed on the Afferent Lymphatic Endothelium, Whereas EMCN Is Present on the Efferent Lymphatics. Expression profiles of those candidate molecules with marked differences between SS and LS both in man and mouse and having antibodies and/or KO animals available were selected for further studies. MSR1, Siglec-1, and EMCN fulfilled those criteria. The fold difference between SS and LS for MSR1 was 26 and for Siglec-1, 18.4. The fold difference between LS and SS for EMCN was 15.4. Also their expression on the cells gated using the same strategy as in cell sorting for the microarray analysis confirmed their presence on LECs. MSR1$^+$ cells formed a separate subpopulation among SS endothelial cells, whereas Siglec-1 and EMCN positivity was seen as a positive shift in SS and LS endothelial cells, respectively (Fig. 1D).

MSR1 and Siglec-1 are well-known macrophage molecules and EMCN is an endothelial molecule also present on stem cells (9, 10). It is difficult to unambiguously discriminate between macrophage and lymphatic endothelial positivity in the SS and occasionally between the lymphatics and blood vasculature using only immunohistochemistry. Therefore, we stained isolated LECs from peripheral and mesenteric lymph nodes (PLNs and MLNs) and analyzed them using flow cytometry. This time we used more markers than in the initial characterization (Fig. 1D) to unambiguously confirm the presence of the markers on LECs. We used double Lyve-1/podoplanin positivity and CD45/CD11b double negativity as the selection criterion, because the LECs are not uniformly positive for both Lyve-1 and podoplanin (Fig. 2A), and they are also present on other CD45$^-$ cell types in LNs (podoplanin for example on fibroblastic reticular cells). The gating strategy to Fig. 2I is shown in Fig. 2 B–H. The results demonstrate that MSR1, Siglec-1, and EMCN are expressed on podoplanin$^+$/CD31$^+$/Lyve-1$^+$ populations with approximate percentages 62.7 ± 5.4 $n = 3$, 7.1 ± 4.8 $n = 3$, and 11.4 ± 8.4 $n = 4$, respectively. Examples are shown in Fig. 2I.

Next we stained PLN and MLN tissue sections using anti-MSR1, anti–Siglec-1, and anti-EMCN antibodies. In PLNs, the MSR1 and Siglec-1 positivity nicely located to the SS. However, MSR1 positivity mainly located to the floor of the SS, whereas Siglec-1$^+$ endothelial cells were occasionally lining the roof, although not in a continuous manner. Neither of them was present in endothelium of LS (Fig. 3A and Fig. S4 A–C). In contrast, EMCN, an endothelial molecule decorated with the MECA 79 epitope and contributing to L-selectin–dependent entrance of lymphocytes into the LNs via high endothelial venules (9, 11) was not present in lymphatic endothelium of the SS, but was present in a subset of Lyve-1 positive and negative LS endothelium in line with the FACS staining shown in Fig. 2I (Fig. 3B).

MLNs drain the gut mucosa and Peyer's patches (PPs) and their afferent lymphatic vessels are in fact efferent lymphatic vessels for PPs. Interestingly, the SS of MLNs were positive for MSR1 and Siglec-1 and their LS negative for these molecules, thus MLNs phenotypically resemble PLNs in this respect (Fig. S4 B–C). Here again, LSs were positive for EMCN, although the expression was less abundant than in PLNs (Fig. S4D). PP sections were double stained with anti-MSR1 or anti–Siglec-1 and anti–Lyve-1. Practically no Siglec-1$^+$ or MSR1$^+$ endothelium was detected (Fig. S4E). In contrast, the Lyve-1$^+$ lymphatic vessels were highly positive for EMCN in agreement with their efferent nature (Fig. S4E).

The expression profiles of MSR1 and Siglec-1 were further tested in skin, where the beginnings of the lymphatics are recognized as blind-ended sacs. Only a subset of lymphatic vessels was found positive for MSR1 and Siglec-1 in immunohistochemistry
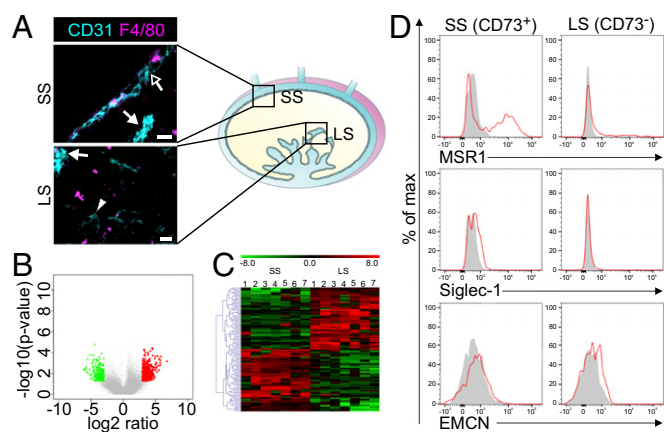

Fig. 1. Transcriptional diversity of SS and LS LECs. (A) SS LECs (CD31$^+$, open arrow) were used as representatives of the afferent arm of the lymphatic vasculature and identified by their position at close proximity to the collagen capsule and incoming macrophages (F4/80$^+$, magenta). LS LECs (CD31$^+$, arrowhead) were used as representatives of the efferent arm of the lymphatic vasculature and identified by their position in the paracortical area. Arrows point to high endothelial venules, which stain more intensively for CD31 than LECs. A schematic drawing shows the LN structure with locations of SS and LS. (Scale bar, 50 µm.) (B) Volcano plot of the microarray data depicting the statistical significance as $-\log_{10} P$ value (y axis) against the fold-change as $\log_2$ ratio (x axis) between LECs of the SS and LS. Genes with $P \leq 0.05$ and the magnitude of expression difference at least eightfold (green, down-regulated; red, up-regulated) are indicated. (C) Heat maps showing the top 100 hierarchially clustered (Euclidean distance, complete linkage) reporters according to the selection LS > SS and LS < SS in seven (one to seven) different isolations (one to five laser dissections, six to seven sorted by flow cytometry). The differentially expressed reporters fulfill the criteria $P \leq 0.05$ and fold-change of ≥8. The expression values are centered to the median $\log_2$ intensity value of all samples and the colors represent the relative expression of a given gene in comparison with the median of all samples. The heat map color scheme with the corresponding $\log_2$ values is given. $n = 7$ in both groups. (D) MSR1, Siglec-1, and EMCN positivity in lineage$^-$/podoplanin$^+$/CD73$^+$ and lineage$^-$/podoplanin$^+$/CD73$^-$ cells (the same gating strategy as used for cell sorting of LECs from SS and LS, and shown in Fig. S1).
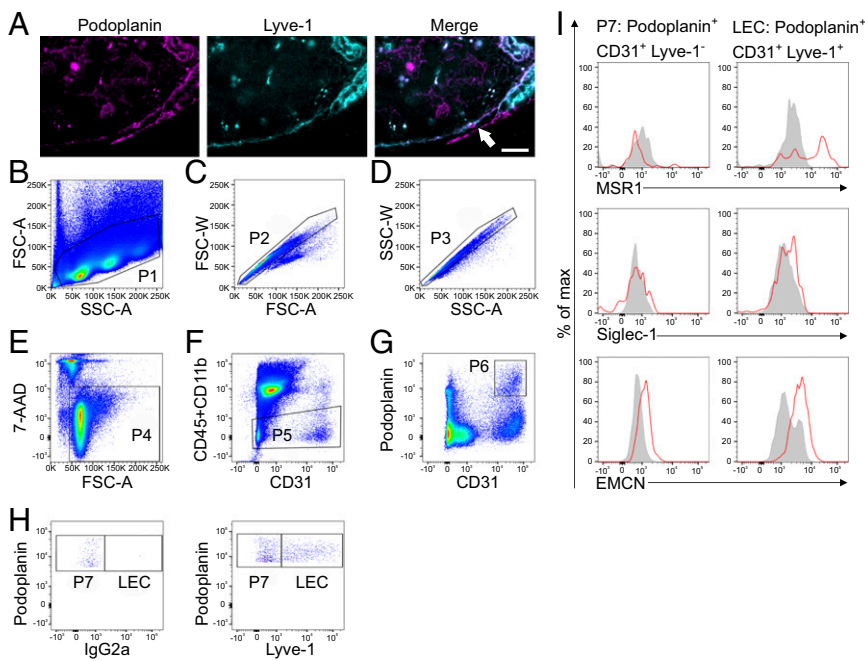
Fig. 2. MSR1, Siglec-1, and EMCN are expressed on LECs. (A) Double staining of mouse LNs with anti–Lyve-1 (cyan) and podoplanin (magenta). The arrow points to podoplanin⁺ and Lyve-1⁻ structures. (Scale bar, 50 μm.) (B–I) Flow cytometric identification of the Lyve-1/podoplanin-1 double positive population used for identification of LECs for analyzing the expression of MSR1, Siglec-1, and EMCN. The starting population (P1 in B) was further gated to exclude aggregated (C and D), dead (E), and CD45⁺, CD11b⁺ cells (F). CD31⁺⁺ and podoplanin⁺⁺ cells (G) were further sorted regarding their Lyve-1 positivity (H). (I) MSR1, Siglec-1, and EMCN (red) positivity was analyzed in podoplanin⁺/CD31⁺/Lyve-1⁺, and podoplanin⁺/CD31⁺/Lyve-1⁻ populations. Staining was carried out with isotype-matched negative control antibodies (gray histograms).

(Fig. 4 *A* and *B*) and especially MSR1 expression was low in the ear skin (Fig. S5*B*). Also isolated LECs (CD45⁻/CD11b⁻/CD31⁺/Lyve-1⁺/podoplanin⁺) had only small subpopulations positive for MSR1 ($23 \pm 6.2\%$, $n = 4$) and Siglec-1 ($25 \pm 6.8\%$, $n = 5$) seen as positive shifts in histograms when isolated from the abdominal and back skin. Examples are shown in Fig. 4*C*.

MSR1 on Lymphatic Endothelium Mediates Binding of Lymphocytes. We first checked whether MSR1 deficiency has an effect on the LN architecture or on its lymphocyte subpopulations. Immunohistochemical and flow cytometric analyses did not reveal any obvious aberrancies between the LNs of KO and WT mice (Fig. 5*A*). Next we used ex vivo frozen section-binding assays to evaluate whether MSR1 on the lymphatic endothelium mediates binding of lymphocytes. As it is practically impossible to discriminate lymphocyte binding to macrophages and LECs in ex vivo frozen section assays, we tested lymphocyte binding to the SS of LNs of clodronate-treated mice after confirming that SS macrophages had been efficiently eliminated, whereas the LECs had retained their clear MSR1 positivity (Fig. 5*B*). In these assays, lymphocytes bound efficiently to the SS and the binding was inhibited with anti-MSR1 antibodies (Fig. 5*C*). The same magnitude of reduction in lymphocyte binding to the SS in clodronate-treated MSR1 KO mice was seen in comparison with their WT controls also treated with clodronate (Fig. 5*C* and Fig. S6*A*). We further confirmed the MSR1-dependent binding using cultured primary mouse LECs and the antibodies found inhibitory in ex vivo adhesion assays. Nearly all Prox-1⁺ LECs were MSR1⁺, although both of these markers were expressed in variable intensity (Fig. 5 *D* and *E*). These assays clearly demonstrated that MSR1 on LECs is able to mediate adhesion of lymphocytes to the endothelium (Fig. 5*E*). Moreover, we created an MSR1-Fc chimera to test adhesive interactions between lymphocytes and MSR1 more directly. This chimera specifically bound to subpopulations of B cells, CD4⁺ and CD11b⁺ cells but not to CD8⁺ cells, indicating that MSR1 can directly bind to leukocytes in a cell-specific manner (Fig. 5*F* and Fig. S6*B*).

MSR1 Controls the Entrance of Lymphocytes to the LN Parenchyma. To test the in vivo significance of MSR1 in lymphocyte traffic, we performed homing assays by injecting lymphocytes to the footpad of MSR1-deficient and WT mice and measured the number and location of fluorescently labeled lymphocytes in the draining LNs. In 12-h homing assays no significant differences were observed in the total number of fluorescently labeled cells or in CD4⁺, CD8⁺, or B cells within the draining LNs between the genotypes (Fig. 5*G* and Fig. S6 *C–E*). Instead, when the distribution of the homed cells within the nodes was analyzed in 4.5-h homing assays by measuring the distance of the arrived cells from the SS, the lymphocytes migrated significantly further in MSR1 KO than in the WT mice (Fig. 5*H* and Fig. S6*F*).

MSR1 Is also Discriminatively Expressed in Human SS and LS and Mediates Lymphocyte Binding. To test how closely the expression patterns of Siglec-1 and MSR1 in mouse resemble those in humans, we used PLNs resected in connection to surgery for head and neck cancer but being macroscopically and microscopically free of cancer. Despite this approach, there was a certain degree of variability in the expression patterns between the donors, most likely reflecting the possibility that the disease has induced aberrant expression of MSR1 and Siglec-1. For further studies, only the nodes having comparable expression patterns with mouse were chosen for functional ex vivo adhesion assays. In these assays, lymphocyte binding both to the SS and LS was measured in the presence and absence of anti-MSR1 and Siglec-1 antibodies (Fig. 5*I*). Anti-MSR1 antibody significantly inhibited the binding of lymphocytes to the SS but no inhibition was seen to the LS. The slight inhibition of lymphocyte binding to SS with anti–Siglec-1 antibody did not reach statistical significance (Fig. 5*I*).

LECs and Macrophages Express SR-AI and SR-AII Variants of MSR1. Human MSR1 has three different transcript variants in macrophages, two being functional scavengers and the third one that has been suggested to regulate the two other ones (12, 13). Like macrophages, also the primary LECs expressed two of the three MSR1 transcript variants, SR-AI and SR-AII (Fig. S7).

Discussion

In this work we were able to show that a multitude of genes are differentially expressed in afferent and efferent lymphatics clearly demonstrating the unique characteristics of these two subtypes of LECs. Even if we only considered genes up- or down-regulated
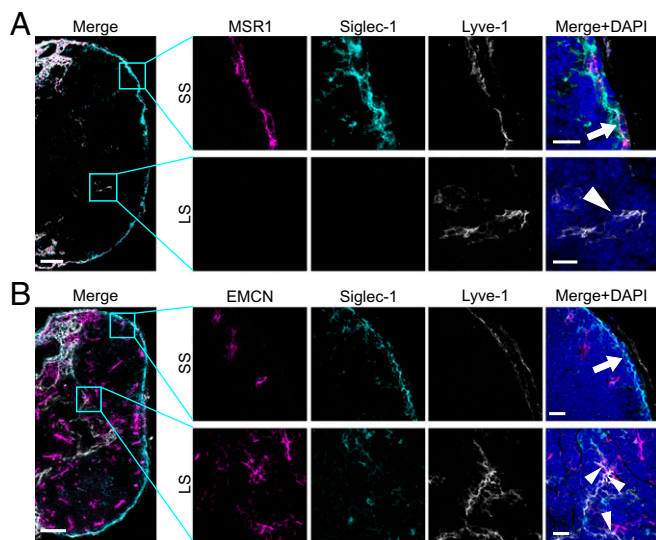
IMMUNOLOGY AND INFLAMMATION

Fig. 3. MSR1 and Siglec-1 are expressed on the SS endothelium and EMCN is expressed on the LS endothelium. (*A* and *B*) Confocal images of MSR1 (magenta), Siglec-1 (cyan), and EMCN (magenta) expression in PLNs. The arrows point to the floor of lymphatic endothelium in SS and the arrowheads to LS (*A* and *B*). Arrowheads in *B* point to double positive regions of LS. [Scale bars, 100 μm (*Left*) and 20 μm (*Insets*).]

more than eightfold, 685 genes fulfilled the criteria of differential expression. These genes belong to a wide variety of categories including genes encoding chemokines, adhesion molecules, growth factors, ion channels, and metabolic pathways. This wide variety strongly suggests that the afferent and efferent endothelial cells are very different in many aspects.

Isolation methods for gene expression analyses both with laser capture microdissection and sorting with flow cytometry have their characteristic limitations, which can cause false positive signals due to contaminating cell populations (14). Laser capture microdissection requires rapid processing in harsh conditions allowing the use of only those antibodies, which give a strong signal and are able to stand the treatment of the tissue. Sorting, on the other hand, needs a combination of different antibodies as none of the antibodies is entirely specific to the lymphatics, and the microanatomical location of the cells cannot be used as a criterion. In addition, cell suspensions containing single endothelial cells are challenging to obtain and the sorting purity is never 100%. For instance, F4/80 is not expressed in all macrophage subpopulations in lymph nodes (15) and CD73 is also present on podoplanin+ fibroblastic reticular cells (16). Therefore, we decided to use both of these isolation methods to collect samples for microarray analysis and select candidate molecules for further studies from those, which were defined as differentially expressed genes when combining samples from both techniques. Nevertheless, the expression of individual genes should be interpreted with caution also in our dataset as in any whole-genome expression study.

MSR1 and Siglec-1 are well-known macrophage molecules and Siglec-1 is especially present on the SS macrophages (17). However, their expression and function on the lymphatics has not been described. Siglec-1 expression is low on lymphatics and more restricted than the expression of MSR1 in the SS being in line with a very low signal (below the cutoff) in IMMGEN analyses (www.immgen.org). MSR1 is a known receptor for acetylated LDL and therefore intimately connected to the development of atherosclerosis (18). To be able to discriminate the function of MSR1 on lymphatics from that on macrophages, we depleted SS macrophages with clodronate. This treatment did not abolish MSR1 on the lymphatic endothelium. Besides being present in the

SS, MSR1 is also expressed on the medullary sinus endothelium (as seen in Fig. 3*A*), but not on cortical or subcortical LS. This is well in line with the report of Braun et al. (19) who found that lymphocytes directly infused into the afferent lymphatics enter the lymph nodes preferentially via the medullary sinus, but use the SS when injected together with dendritic cells.

Besides acetylated LDL, MSR1 on macrophages has additional ligands and can bind a wide variety of bacteria. It also mediates macrophage adhesion to the culture surfaces in vitro (20), thus demonstrating its adhesive properties. We could show that lymphocytes bind to the SS in an MSR1-dependent manner and LECs can support adhesion of lymphocytes, thus revealing the functional importance of this molecule in cell–cell interaction. We also tested a possible role for MSR1 in overall homing of footpad-injected lymphocytes via the afferent lymphatics, but could not see any difference between WT and KO animals, when we analyzed the number of homed cells by flow cytometry. This is consistent with the expression pattern of MSR1 that is scarce in the afferent lymphatic vessels in the skin and becomes abundant only in the SS. Therefore, we analyzed the fate of the LN-arrived cells and found them to travel significantly further in the LN parenchyma of KO mice than in their WT controls at early time points, when the cells are not yet dispersed throughout the LNs. Although the MSR1 on macrophages can also contribute to this traffic, the results of ex vivo and in vitro adhesion assays indicate a direct contribution of
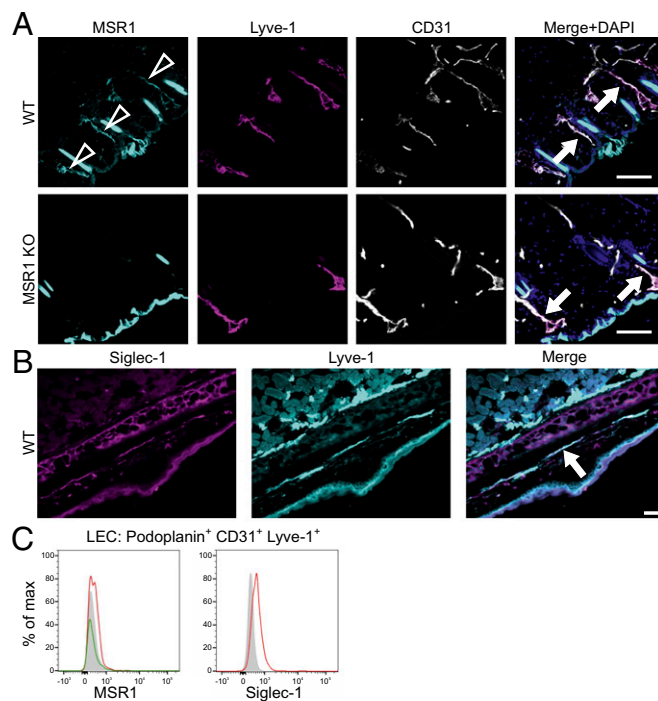

Fig. 4. Expression of MSR1 and Siglec-1 is scarce in mouse skin. (*A*) Quadruple immunostaining of WT and MSR1 KO mice for MSR1 (cyan), Lyve-1 (magenta), CD31 (white), and DAPI (blue). The arrowheads point to MSR1+ vessels and the arrows point to double and triple positive vessels. The positivity of the keratinocyte layer and hair follicles in MSR1 staining (cyan, green channel in the original staining) is nonspecific and seen also in KO samples. The images are representative of at least five samples per group. (Scale bars, 100 μm.) (*B*) Double immunostainings of WT mice for Siglec-1 (magenta) and Lyve-1 (cyan). The arrow points to one double positive vessel as an example. (Scale bar, 50 μm.) (*C*) Flow cytometric analyses of MSR1 and Siglec-1 expression of isolated LECs from the skin. The gating of the CD45⁻/CD11b⁻/CD31+/Lyve-1+/podoplanin+ population is shown in Fig. S5A. The expression of the indicated molecules in WT is shown as red histograms and MSR1 KO as green histograms; gray histograms are stainings with isotype-matched negative control antibodies.

Fig. 5. MSR1 mediates lymphocyte binding to the lymphatic endothelium and is involved in lymphocyte entrance to the LN parenchyma. (*A*) Immunofluorescence staining of popliteal LNs of WT and MSR1 KO mice with lymphocyte markers for B- and T-cell subpopulations and endothelial markers (*Left*) demonstrating the normal appearance of the LNs in MSR1 KO mice. (Scale bar, 250 μm.) Lymphocyte subpopulations quantified by FACS from popliteal LNs of WT and MSR1 KO mice (*n* = 39 WT and 40 KO, *Right*). (*B*) Expression of MSR1 in popliteal LNs of WT mice treated with control liposomes (*Upper*) and clodronate-containing liposomes (*Lower*), nuclear staining with DAPI (blue) in merge. Arrows point to Siglec-1^{+} macrophages absent after clodronate treatment. (Scale bar, 20 μm.) (*C*) Ex vivo adhesion: binding of lymphocytes was tested to SS in frozen sections of popliteal LNs from clodronate-treated WT and MSR1 KO mice and after incubation with anti-MSR1 control antibodies to clodronate-treated WT lymph nodes. The results are presented as mean ± SEM and are pooled from three independent experiments. (*D*) Expression of MSR1 on cultured primary LECs (*Left*) using four-color immunofluorescence stainings. (Scale bar, 50 μm.) (*E*) Lymphocyte binding to cultured primary LECs using anti-MSR1 and control antibodies for inhibition. An example of the adhesion is shown on the *Right*; lymphocytes (cyan, few indicated by arrows) are binding to a monolayer of LECs stained by anti-podoplanin (white). DAPI (blue) indicates the nuclei. (Scale bar, 50 μm.) (*F*) Binding of MSR1-Fc chimera to different subpopulations of B cells, CD4, CD8, and CD11b positive cells analyzed by FACS. Percentages and relative intensity of the binding (measured as mean fluorescence intensity) of MSR1-Fc chimera are shown. Binding of the control is set to 1.0 by definition, *n* = 4. (*G*) Relative homing of footpad-injected CFSE[+] lymphocytes into the draining LNs of WT and MSR1 KO mice in 12-h migration experiments (*Left*) and relative portion of lymphocyte subpopulations from migrated CFSE^{+} cells (*Right*). Data are pooled from five experiments. WT is set to 1.0 by definition. (*H*) Average distance of migrated CFSE^{+} cells from the SS in 4.5-h migration experiments. Data are pooled from two experiments (*n* = 11 WT and 10 MSR1 KO mice, from which 211 (WT sections) and 233 (MSR1 KO sections) cells were measured. Data are presented as mean ± SEM (*I*) Lymphocytes binding to the SS and LS in a human LN section. (*Left*) Some of the bound cells are pointed out by arrows; the focus is always a compromise with the bound cells and the tissue, dark field. SS and LS are outlined by dashed line. C, capsule of the LN. (Magnification: 200×.) (*Right*) Quantification of lymphocyte binding to the SS and LS in ex vivo adhesion assays in the presence of anti-MSR1, anti-Siglec-1, or negative control antibodies. Binding in the presence of the control antibodies is set to 100% by definition. The bars represent the combined results from three separate experiments as mean ± SEM *P ≤ 0.05, **P ≤ 0.01, ***P ≤ 0.001.
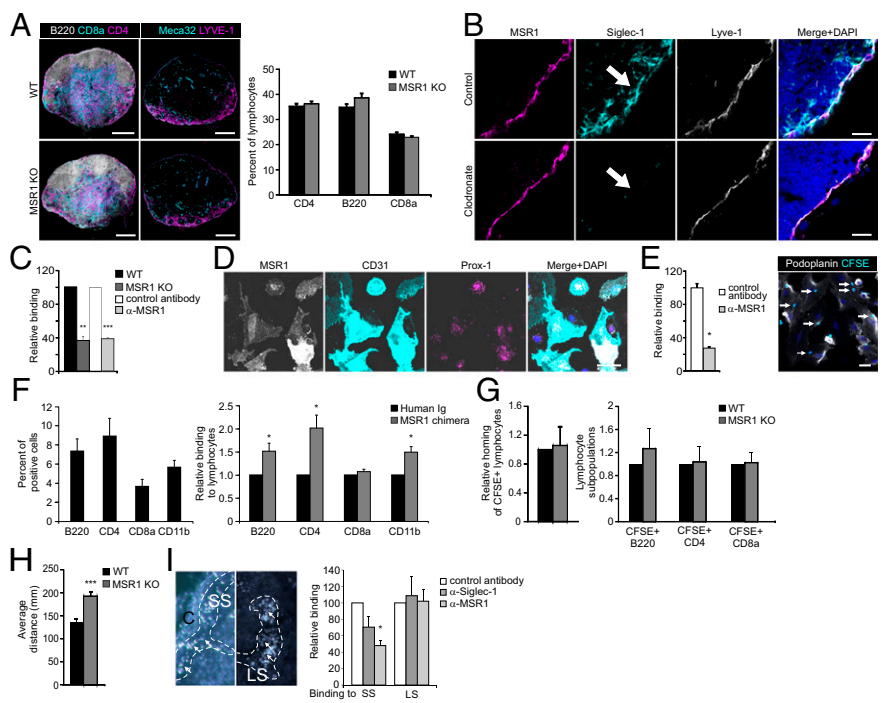
lymphatic MSR1 in this process. As we also were able to demonstrate direct binding of recombinant MSR1 to lymphocytes, we interpret the results so that lymphocytes interact with LECs involving adhesion mediated by MSR1 and this process slows down the entrance of lymphocytes from the SS to lymph node parenchyma. Many cancer types, as for example breast and head and neck cancers, prefer the lymphatics as the route for metastasizing. Therefore, it could be envisioned that MSR1 may also be involved in cancer cell entrance into the lymph nodes.

An interesting terminological question is: What is the nature of the lymphatics leaving the PPs and entering the MLNs, as the same vessels are efferent for PPs and afferent for the MLNs? The lack of MSR1 and Siglec-1 on the lymphatics of PPs and their appearance on the lymphatics when approaching the MLNs indicate phenotypical and location-dependent heterogeneity within a lymphatic vessel, which matches well with the selective expression of MSR1 and Siglec-1 on the afferent lymphatics. Moreover, the abundant expression of EMCN on PP lymphatics is in line with their efferent nature.

One of the fundamental functional differences between LECs is that the afferent lymphatic endothelium interacts with several leukocyte subtypes, whereas endothelial cells in the efferent lymphatics only mediate lymphocyte trafficking. Theoretically, this may be due to the trapping of other leukocytes by the structures within the nodes or lack of appropriate traffic signals and molecules in efferent lymphatics. In the list of differentially expressed genes, few molecules are known to participate in intra-organ and/or cell trafficking via blood vessels (21, 22) and may potentially be involved in the selective trafficking in the different arms of the lymphatic system as well. Such molecules are for

example CCL12 and CCL19. On the other hand, there are some unexpected candidates such as for example the β2-adrenergic receptor that has been recently described as an important receptor on lymphocytes regulating lymphocyte egress from LNs by enhancing retention-promoting signals through CCR7 and CXCR4 (23). Preferential expression of the β2-adrenergic receptor on the lymphatic endothelium of the SS in our analyses suggests that it may also have a role in the lymphatics.

In this work, we have elucidated the differences between the afferent and efferent arms of LECs within the LNs. The results revealed marked differences in gene expression of many molecular categories and pathways reflecting their functional differences. These newly identified differences may provide targets for drug development to manipulate lymphangiogenesis, cellular traffic, as well as metabolic and fluid balance to control different disease entities.

Methods

Mice. C57BL/6J WT and MSR KO mice were from The Jackson Laboratory. All animal experiments were approved by the Ethical Committee for Animal Experimentation in Finland.

Laser-Capture Microdissection and Pressure Catapulting. Laser-capture microdissection and pressure catapulting (LCMP) was conducted on a PALM microbeam instrument. Murine peripheral LNs were used for isolation of LECs from SS and LS. To maximize the collection of the right cells, the sections were stained with Alexa Fluor 488 anti-mouse CD31 and PE-Texas Red anti-mouse F4/80 antibodies and in SS and LS only discrete CD31^{+} cells were collected (see Table S3 for detailed information about antibodies).

Isolation and Sorting of LECs. Peripheral LNs and MLNs were digested with liberase and DNase I. For cell sorting the following antibodies were used:

IMMUNOLOGY AND INFLAMMATION

allophycocyanin (APC)-conjugated lineage mixture, PE anti-CD73, and PE/Cy7 anti-podoplanin. For primary cell cultures, mouse PLNs and MLNs were digested with collagenase P and neutral protease. After 7 d, CD45$^-$/CD11b$^-$/podoplanin$^+$/CD31$^+$/Lyve-1$^+$ cells were sorted with FACSAria IIu.

Microarray Analyses. RNA amplification, labeling, and cDNA microarray hybridization and gene expression analyses were performed at the Miltenyi Biotec Genomic Services. The sorted cells were subjected to SuperAmp RNA amplification. The Cy3-labeled cDNAs were hybridized to Agilent Whole Mouse Genome Oligo Microarrays 8× 60 K. Fluorescence signals of the hybridized Agilent microarrays were detected using Agilent's Microarray Scanner System. The Agilent Feature Extraction Software (FES) was used to process the microarray image files. The microarray data have been submitted to GEO archive (GSE 68371).

In bioinformatics analyses, the differential gene expression between the SS and LS of the LCM samples were tested with a one-way ANOVA and an adjusted P value was calculated by the method of Benjamini and Hochberg (24). All samples of the LS and SS populations were further used as a test and reference group, respectively, by performing Student's t test (two tailed). The differentially expressed (DE) genes were selected requiring a fold-change above two- or eightfold and $P < 0.05$. A detection P value (Rosetta resolver error model) (25) was also calculated for each reporter.

Functional grouping analyses were performed using the differentially expressed genes as input gene populations. The annotations were derived from Gene Ontology databases and various other pathway resources curated by Miltenyi Biotec. The differentially expressed reporters were tested for significant enrichments of annotations using the TreeRanker software (Miltenyi). The frequency of the association of a category with the input reporter set was compared with that of a background set (Agilent 8 × 60 K array genes). P values were computed by Fisher's exact test with Benjamini–Hochberg correction for multiple testing. The data were further analyzed using the GENE-E analysis platform (https://www.broadinstitute.org/cancer/software/GENE-E/).

Immunohistochemical Analyses. Frozen sections were stained with primary antibodies against mouse CD204, CD169, EMCN, Lyve-1, podoplanin/gp36, and PLVAP-1 (Meca 32) followed by relevant second-stage reagents. The following direct conjugates were used: Alexa Fluor 647 anti-CD4, Pacific Blue anti-CD45R, Alexa Fluor 488 anti-CD8, Alexa Fluor 488 anti-CD204, and Alexa Fluor 488 anti–Lyve-1. Alternatively, paraffin-embedded LN sections were stained with primary antibodies against Lyve-1 and podoplanin/gp36 with proper second-stage reagents. Primary mouse LECs (MLECs) were stained with directly conjugated primary antibodies: Alexa Fluor 647 anti-CD204, Alexa Fluor 488 anti-CD31, and unconjugated anti-PROX1.

Flow Cytometric Analyses. The following primary, secondary, and isotype control antibodies were used against mouse: APC-Cy7 anti-CD45, APC-Cy7 anti-CD11b, PE/Cy7 anti-podoplanin, APC anti-CD31, PE anti–Lyve-1, eFluor 660 anti-EMCN, anti-CD204, anti-CD169, anti-EMCN with proper controls. Cells were analyzed on a FACSAria and LSR Fortessa using FlowJo software.

Adhesion Assays.
Ex vivo. In principle the adhesion assays were performed as described earlier (26). The number of lymphocytes bound to SS and LS was counted under dark-field microscopy. To be able to standardize day-to-day variations between the experiments, binding to the control sections was set to 100% by definition. Macroscopically and microscopically normal LNs from three anonymous human donors (obtained from surplus tissue from surgical operations) and blood samples for lymphocyte purification from healthy volunteers (informed consent obtained) with the permission of the Ethical Committee of Turku University Hospital and three different KO and WT mice were used.
In vitro 1. MSR1-Ig chimera and control Ig were incubated with mouse lymphocytes and the binding was detected using biotin-conjugated anti-human Ig Fc followed by Alexa Fluor 488 streptavidin. Statistical analyses were performed using the Mann-Whitney u test.
In vitro 2. Lymphocyte binding to primary MLECs was tested as previously described (27).

Lymphocyte Migration in Vivo. Carboxyfluorescein diacetate succinimidyl ester (CFSE)-labeled lymphocytes were injected subcutaneously into the hind paws of WT or MSR1 KO mice. After 12 h or 4.5 h the draining popliteal LNs were collected for further analyses. Single cell suspensions of the LNs for flow cytometry were stained with the lymphocyte markers for CD45R, CD4, and CD8a. Unfixed frozen sections were stained with anti-mouse Lyve-1. The shortest distance of each CFSE$^+$ cell in the LN parenchyma from SS was measured manually using Zen2012 (Carl Zeiss). Statistical analyses were performed using the Mann–Whitney u test.

Macrophage Depletion. SS macrophages were depleted by subcutaneous injections of clodronate or control liposomes (28) to the footpads.

Statistical Analyses. Statistical analyses used have been indicated in each methodological description if not two-tailed Student's t test and the P values have been presented in figures/figure legends.

1. Mumprecht V, Detmar M (2009) Lymphangiogenesis and cancer metastasis. *J Cell Mol Med* 13(8A):1405–1416.
2. Johnson LA, Jackson DG (2008) Cell traffic and the lymphatic endothelium. *Ann N Y Acad Sci* 1131:119–133.
3. Rosen H, Sanna G, Alfonso C (2003) Egress: A receptor-regulated step in lymphocyte trafficking. *Immunol Rev* 195:160–177.
4. Ledgerwood LG, et al. (2008) The sphingosine 1-phosphate receptor 1 causes tissue retention by inhibiting the entry of peripheral tissue T lymphocytes into afferent lymphatics. *Nat Immunol* 9(1):42–53.
5. Marttila-Ichihara F, et al. (2008) Macrophage mannose receptor on lymphatics controls cell trafficking. *Blood* 112(1):64–72.
6. Karikoski M, et al. (2009) Clever-1/Stabilin-1 regulates lymphocyte migration within lymphatics and leukocyte entrance to sites of inflammation. *Eur J Immunol* 39(12):3477–3487.
7. Fletcher AL, et al. (2011) Reproducible isolation of lymph node stromal cells reveals site-dependent differences in fibroblastic reticular cells. *Front Immunol* 2:35.
8. Ålgars A, et al. (2011) Different role of CD73 in leukocyte trafficking via blood and lymph vessels. *Blood* 117(16):4387–4393.
9. Samulowitz U, et al. (2002) Human endomucin: Distribution pattern, expression on high endothelial venules, and decoration with the MECA-79 epitope. *Am J Pathol* 160(5):1669–1681.
10. Matsubara A, et al. (2005) Endomucin, a CD34-like sialomucin, marks hematopoietic stem cells throughout development. *J Exp Med* 202(11):1483–1492.
11. Kanda H, et al. (2004) Endomucin, a sialomucin expressed in high endothelial venules, supports L-selectin-mediated rolling. *Int Immunol* 16(9):1265–1274.
12. Matsumoto A, et al. (1990) Human macrophage scavenger receptors: Primary structure, expression, and localization in atherosclerotic lesions. *Proc Natl Acad Sci USA* 87(23):9133–9137.
13. Gough PJ, Greaves DR, Gordon S (1998) A naturally occurring isoform of the human macrophage scavenger receptor (SR-A) gene generated by alternative splicing blocks modified LDL uptake. *J Lipid Res* 39(3):531–543.
14. Espina V, et al. (2006) Laser-capture microdissection. *Nat Protoc* 1(2):586–603.
15. Gray EE, Cyster JG (2012) Lymph node macrophages. *J Innate Immun* 4(5–6):424–436.
16. Yegutkin GG, et al. (2015) Ecto-5′-nucleotidase/CD73 enhances endothelial barrier function and sprouting in blood but not lymphatic vasculature. *Eur J Immunol* 45(2):562–573.
17. Phan TG, Green JA, Gray EE, Xu Y, Cyster JG (2009) Immune complex relay by subcapsular sinus macrophages and noncognate B cells drives antibody affinity maturation. *Nat Immunol* 10(7):786–793.
18. de Winther MP, van Dijk KW, Havekes LM, Hofker MH (2000) Macrophage scavenger receptor class A: A multifunctional receptor in atherosclerosis. *Arterioscler Thromb Vasc Biol* 20(2):290–297.
19. Braun A, et al. (2011) Afferent lymph-derived T cells and DCs use different chemokine receptor CCR7-dependent routes for entry into the lymph node and intranodal migration. *Nat Immunol* 12(9):879–887.
20. Suzuki H, et al. (1997) A role for macrophage scavenger receptors in atherosclerosis and susceptibility to infection. *Nature* 386(6622):292–296.
21. Jia GQ, et al. (1996) Distinct expression and function of the novel mouse chemokine monocyte chemotactic protein-5 in lung allergic inflammation. *J Exp Med* 184(5):1939–1951.
22. Förster R, Davalos-Misslitz AC, Rot A (2008) CCR7 and its ligands: Balancing immunity and tolerance. *Nat Rev Immunol* 8(5):362–371.
23. Nakai A, Hayano Y, Furuta F, Noda M, Suzuki K (2014) Control of lymphocyte egress from lymph nodes through β2-adrenergic receptors. *J Exp Med* 211(13):2583–2598.
24. Benjamini Y, Hochberg Y (1995) Controlling the false discovery rate: A practical and powerful approach to multiple testing. *J R Stat Soc B* 57(1):289–300.
25. Weng L, et al. (2006) Rosetta error model for gene expression analysis. *Bioinformatics* 22(9):1111–1121.
26. Irjala H, et al. (2001) Mannose receptor is a novel ligand for L-selectin and mediates lymphocyte binding to lymphatic endothelium. *J Exp Med* 194(8):1033–1042.
27. Airas L, et al. (1995) CD73 is involved in lymphocyte binding to the endothelium: Characterization of lymphocyte-vascular adhesion protein 2 identifies it as CD73. *J Exp Med* 182(5):1603–1608.
28. Van Rooijen N, Sanders A (1994) Liposome mediated depletion of macrophages: Mechanism of action, preparation of liposomes and applications. *J Immunol Methods* 174(1–2):83–93.

Iftakhar-E-Khuda et al.